(b) V. B. Koutecky and J. I. Musher, *Theor. Chim. Acta*, **33**, 227 (1974); (c) N. Rösch, V. H. Smith, and M.-H. Whangbo, *Inorg. Chem.*, **15**, 1768 (1976); (d) P. J. Hay, *J. Am. Chem. Soc.*, **99**, 1003 (1977); (e) R. D. Brown and J. B. Peel, *Aust. J. Chem.*, **21**, 2605, 2617 (1968); (f) L. Radom and H. F. Schaeffer III, *Aust. J. Chem.*, **28**, 2069 (1975); (g) A. H. Cowley, M. Lattman, and M. L. Walker, *J. Am. Chem. Soc.*, **101**, 4074 (1979).
(5) (a) J. Kapovits and A. Kálmán, *Chem. Commun.*, 649 (1971); (b) A. Kálmán, K. Sasvári, and I. Kapovits, *Acta Crystallogr., Sect. B*, **29**, 355 (1973).
(6) E. F. Perozzi, J. C. Martin, and I. C. Paul, *J. Am. Chem. Soc.*, **96**, 6735 (1974).
(7) L. J. Adzima, E. N. Duesler, and J. C. Martin, *J. Org. Chem.*, **42**, 4001 (1977).
(8) K. C. Hodges, D. Schomburg, J.-V. Weiss, and R. Schmutzler, *J. Am. Chem. Soc.*, **99**, 6096 (1977).
(9) L. J. Adzima, C. C. Chiang, I. C. Paul, and J. C. Martin, *J. Am. Chem. Soc.*, **100**, 953 (1978).
(10) M. W. Tolles and W. D. Gwinn, *J. Chem. Phys.*, **36**, 1119 (1962).
(11) (a) K. Kimura and S. H. Bauer, *J. Chem. Phys.*, **39**, 3172 (1963); (b) V. C. Ewing and L. E. Sutton, *Trans. Faraday Soc.*, **59**, 1241 (1963).
(12) N. C. Baenzinger, R. E. Buckles, R. J. Maner, and T. D. Simpson, *J. Am. Chem. Soc.*, **91**, 5749 (1969).
(13) (a) I. C. Paul, J. C. Martin, and E. F. Perozzi, *J. Am. Chem. Soc.*, **93**, 6674 (1971); (b) *ibid.*, **94**, 5010 (1972).
(14) (a) L. N. Markovski, V. E. Pashinnik, and A. V. Kirsanov, *Synthesis*, 787 (1973); (b) L. N. Markovski and V. E. Pashinnik, *ibid.*, 801 (1975); (c) W. J. Middleton, *J. Org. Chem.*, **40**, 574 (1975).
(15) A. H. Cowley, D. J. Pagel, and M. L. Walker, *J. Am. Chem. Soc.*, **100**, 7065 (1978).
(16) P. E. Riley and R. E. Davis, *Acta Crystallogr., Sect. B*, **32**, 381 (1976).
(17) "International Tables for X-ray Crystallography", Vol. IV, Kynoch Press, Birmingham, England, 1974.
(18) R. F. Stewart, E. R. Davidson, and W. T. Simpson, *J. Chem. Phys.*, **42**, 3175 (1965).
(19) See paragraph at end of paper regarding supplementary material.
(20) E. L. Muetterties and R. A. Schunn, *Q. Rev., Chem. Soc.*, **20**, 245 (1966).
(21) (a) G. C. Demitras, R. A. Kent, and A. G. MacDiarmid, *Chem. Ind. (London)*, **41**, 1712 (1964); (b) G. C. Demitras and A. G. MacDiarmid, *Inorg. Chem.*, **6**, 1903 (1967); (c) S. P. von Halasz and O. Glemser, *Chem. Ber.*, **103**, 594 (1970); (d) *ibid.*, **104**, 1247 (1971).
(22) The nature of the sulfur "lone pair" in SF_4 and its cognates is not a simple matter. For a discussion of this aspect see, for example, ref 4g.
(23) (a) I. G. Csizmedia, A. H. Cowley, M. W. Taylor, L. M. Tel, and S. Wolfe, *J. Chem. Soc., Chem. Commun.*, 1147 (1972); (b) A. H. Cowley, M. W. Taylor, M.-H. Whangbo, and S. Wolfe, *ibid.*, 838 (1976); (c) I. G. Csizmadia, A. H. Cowley, M. W. Taylor, and S. Wolfe, *ibid.*, 432 (1974); (d) A. H. Cowley, D. J. Mitchell, M.-H. Whangbo, and S. Wolfe, *J. Am. Chem. Soc.*, in press.
(24) We thank a reviewer for this suggestion.
(25) The sum of angles at each nitrogen atom is 357.4 ± 2.4°. The dihedral angle between each CNC plane and the equatorial plane is 70.1 ± 2.7°. See: H. Oberhammer and R. Schmutzler, *J. Chem. Soc., Dalton Trans.*, 1454 (1976). The conformation **5** was predicted earlier on the basis of UV photoelectron spectroscopic measurements. See: A. H. Cowley, M. J. S. Dewar, D. W. Goodman, and J. R. Schweiger, *J. Am. Chem. Soc.*, **95**, 6506 (1973).
(26) L. Pauling, "The Nature of the Chemical Bond", 3rd ed., Cornell University Press, Ithaca, N.Y., 1960.
(27) W. H. Baur, *Acta Crystallogr., Sect. B*, **28**, 1456 (1972).
(28) L. Battelle, C. Knobler, and J. D. McCullough, *Inorg. Chem.*, **6**, 958 (1967).
(29) C. Knobler and J. D. McCullough, *Inorg. Chem.*, **11**, 3026 (1972).
(30) W. C. Hamilton and J. A. Ibers, "Hydrogen Bonding in Solids", W. A. Benjamin, New York, 1968, Chapter 2.

EXAFS Studies of Proteins and Model Compounds Containing Dimeric and Tetrameric Iron–Sulfur Clusters

Boon-Keng Teo,*[1a] R. G. Shulman,*[1a] G. S. Brown,[1b] and A. E. Meixner[1a]

Contribution from Bell Laboratories, Murray Hill, New Jersey 07974.
Received January 2, 1979

Abstract: Proteins and model compounds containing dimeric and tetrameric iron–sulfur clusters have been studied by extended X-ray absorption fine structure (EXAFS) spectroscopy in fluorescence and transmission modes. Iron–sulfur and iron–iron distances have been obtained for both proteins and models. Debye–Waller factors, accurate to within 10%, provide an indirect but reliable measure of the spread of these distances. Detailed comparisons of these molecular parameters (average interatomic distances and Debye–Waller factors) are made between (1) proteins and models (which provides direct structural evidence that Holm's model compounds are excellent representations of the active sites of the proteins); (2) solid and solution states (which shows no drastic structural changes at the active site upon dissolution of the proteins); (3) oxidized and reduced states (which reveals small but significant structural changes upon redox). Thus, the present study bridges the two reservoirs of structural information on these important nonheme iron–sulfur proteins—the intact protein on one hand and the bare inorganic clusters on the other. It also provides strong evidence that structural changes at the active site(s) are energetically insignificant as judged by comparing the protein structures with those of the model compounds.

Introduction

The class of nonheme iron–sulfur proteins has been shown to be involved in a variety of biological reactions including photosynthesis, nitrogen fixation, and mammalian steroid hydroxylation. These metalloproteins function as electron carriers via their redox reactions. There are four prototypes of the nonheme iron–sulfur proteins containing one, two, four, or eight iron atoms. The corresponding prosthetic groups are $Fe(SR)_4$ in rubredoxins; $Fe_2S_2{}^*(SR)_4$ for plant, mammalian, and certain bacterial ferredoxins (Fd); $Fe_4S_4{}^*(SR)_4$ for photosynthetic "high-potential" iron proteins (HIPIP) and nonphotosynthetic bacterial ferredoxins; and two $Fe_4S_4{}^*(SR)_4$ units for bacterial ferredoxins where S* and SR refer to sulfide and cysteinyl moieties, respectively.[2]

Extensive chemical and physical data have been obtained for these metalloproteins. X-ray protein crystallography[3,4] has provided structural information on several of the iron–sulfur proteins. The resolution, generally about 2.0 Å, has not been good enough to evaluate accurately the structural changes of the iron–sulfur clusters upon reduction. On the other hand, Holm and co-workers have synthesized a class of organometallic analogues of the active sites of the four types of iron–sulfur proteins which can serve as detailed structural models.[5-7] We consider it of the utmost importance to bridge these two reservoirs of structural information on iron–sulfur proteins: the intact protein on one hand and the bare inorganic cluster models on the other. Such a linkage would be highly significant by allowing a detailed assessment on the extent to which the intrinsic properties, and hence the biological functions, of the active sites are modified by the proteins.

Recently we have reported comprehensive extended X-ray absorption fine structure (EXAFS) studies on rubredoxin and its model compounds in the oxidized and reduced states.[8] Rubredoxin is a particularly favorable compound for EXAFS

0002-7863/79/1501-5624$01.00/0 © 1979 American Chemical Society

study in that it contains one iron atom bonded to four cysteinyl sulfurs such that its EXAFS spectrum is dominated by backscattering from the four nearest-neighbor sulfur atoms.[8,9] The X-ray crystallographic result had been interpreted as showing that one of the four iron-sulfur distances in oxidized rubredoxin was substantially shorter than the other three (2.05 (3) vs. 2.30 (av) Å),[3a-c] which suggested a mechanism for regulating the redox potential by straining an iron-sulfur bond length. We found by the EXAFS experiments that there is no very short bond in oxidized rubredoxin and that the four iron-sulfur distances have a root mean square spread which, if we assume a model where three bonds have a distance R_3 and one R_1, converts into $|R_3 - R_1| = 0.04$ (+0.06 and −0.04) Å. Furthermore, the EXAFS measurements showed that the oxidized and reduced states of rubredoxin had essentially the same structures as the corresponding states of Holm's model.[5]

As a continuation of the effort to acquire accurate structural information about this class of iron-sulfur proteins, we now report EXAFS studies on the ferredoxins containing dimeric and tetrameric iron-sulfur clusters and their model compounds in various oxidation states. There are several reasons for the present study. First, it provides accurate structural parameters for the prosthetic groups in the proteins. Second, by studying different proteins and their corresponding model compounds simultaneously we were able to compare their structures. Our results show that Holm's models are excellent structural representations of the active sites of these proteins thereby confirming and augmenting many other physiochemical comparisons. Third, EXAFS studies on ferredoxins in different oxidation states allow a quantitative evaluation of the effects of strain energy at the active site structures upon the redox reactions. Fourth, the capability of EXAFS spectroscopy to provide structural information on the proteins in solution is used to show that, within the accuracy of these structural determinations, no changes are observed between solution and powder structures of the iron-sulfur prosthetic groups.

Experimental Section

Materials. The model compounds $(Et_4N)_2^+[FeS(SCH_2)_2C_6H_4]_2^{2-}$ and $(Et_4N)_2^+[FeS(SCH_2Ph)]_4^{2-}$ were prepared according to Holm's methods.[6,7] The experiments were performed on these microcrystalline solids loaded in a drybox and sealed with thin Kapton tape (1 mil). The cells (1-3 × 2 × 30 mm³) were kept under an inert atmosphere until just prior to measurements. A comparison of successive scans indicated that sample degradation due to radiation damage or air oxidation was minimal. The proteins were prepared by N. A. Stombaugh, L. L. Anderson, and C. C. McDonald of the E. I. du Pont Central Research and Development Department and kindly given to us for these experiments. Rhubarb ferredoxin[10] was prepared by modification of the procedures reported by Petering and Palmer and by Kerestes-Nagy and Margoliash. The concentrated, lyophilized pineapple variety rhubarb ferredoxin had a purity index of A_{420}/A_{275} = 0.46. HIPIP was prepared by a slight adaptation of Bartsch's published procedure.[11a] At the end the column fractions having $A_{388}/A_{283} \geq 0.38$ were pooled and frozen after concentration for the EXAFS sample. *C. pasteurianum* ferredoxin was prepared by the method of Mortenson, Valentine, and Carnahan.[11b]

X-ray Absorption Measurements. All X-ray absorption measurements described herein were performed at Stanford Synchrotron Radiation Laboratory (SSRL) using the synchrotron radiation from Stanford Positron Electron Accelerating Ring (SPEAR) at Stanford Linear Accelerator Center (SLAC).[12] The EXAFS I spectrometer constructed by Kincaid, Eisenberger, and Sayers was used for these measurements.[13] The model compounds were measured with the transmission technique. The X-ray beam (slit = 1 × 20 mm²) from SPEAR, after being made monochromatic by a channel-cut silicon crystal, passes through the first ionization chamber which measures the incident beam intensity I_0, then through the sample, and finally through another ionization chamber which measures the transmitted intensity I. Nitrogen was the detecting gas used in both ionization chambers. The EXAFS spectra were typically recorded with an integration time of 2 s/point with 400 steps covering about 800 eV above the edge. On the other hand, the proteins were studied with the fluorescence technique,[14] which is almost an order of magnitude more sensitive than the transmission method for dilute systems such as metalloenzymes. The fluorescence detector was a nine-element array of NaI detectors each designed to count up to a rate of 200 000 Hz without significant saturation. This detector, oriented at 90° to the incident beam and in the horizontal plane, registered Kα and Kβ fluorescence X-rays from the iron atoms as well as background Compton and Rayleigh scattered photons. The scattered radiation is weakest at 90° in the horizontal plane, owing to the strong linear polarization of the X-ray beam. However, because of the finite acceptance angle of the spectrometer, each detector has a unique background rate, determined by its angular position, and a unique signal-to-noise ratio. Therefore, a weighted sum was performed so as to maximize the overall signal-to-noise ratio. Data were accumulated at energy intervals of 1.0 eV. The dwell time was 1.0 s/point in all cases, and each scintillation counter operated at a rate between 100 and 200 kHz. Test measurements performed on heme compounds at even higher rates proved that counter saturation effects were negligible (P. Eisenberger, private communication).

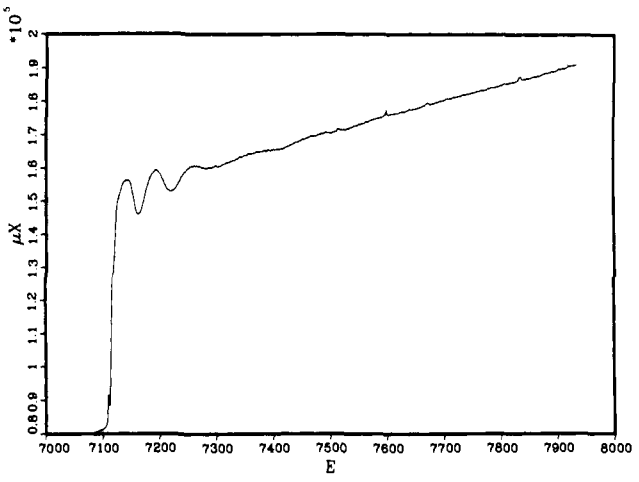

Figure 1. X-ray fluorescence data of oxidized bacterial ferredoxin in solution.

Data Analysis

Data Reduction. The raw data were accumulated in intervals uniformly spaced in monochromator angle which were subsequently converted to photon energy E. This is the abscissa of the spectra. The ordinates of the spectra are computed by taking $\mu x = \ln I_0/I$ for the transmission data or $= I_0/F$ for the fluorescence data. Here, μ is the total absorption coefficient, x is the sample thickness, I_0 and I, which are proportional to the incident and the transmitted beam intensities, were measured by the first and the second ionization chambers, respectively, and F is the fluorescence intensity measured by the scintillation counters. Figure 1 shows a typical plot of μx vs. E at and above the iron K edge of the oxidized bacterial ferredoxins in solution. For EXAFS analysis, it is necessary to convert the photon energy E into photoelectron wave vector

$$k = \left[\frac{2m}{\hbar^2}(E - E_0)\right]^{1/2} \quad (1)$$

where E_0 is the energy threshold of the iron K edge and m is the mass of an electron. We use parametrized theoretical amplitude and phase functions[15] in the analysis and do not let them vary. We allow the energy threshold E_0 to vary from its starting value, which was chosen at 7127 eV.[16] The reason is that the arbitrarily chosen E_0 may not be consistent with the theoretical phase shifts. After conversion to k space, the data were multiplied by k^3 and the background, due in large part to ligand absorption, Compton scattering, and the changes of ionization chamber efficiency with photon energy, was re-

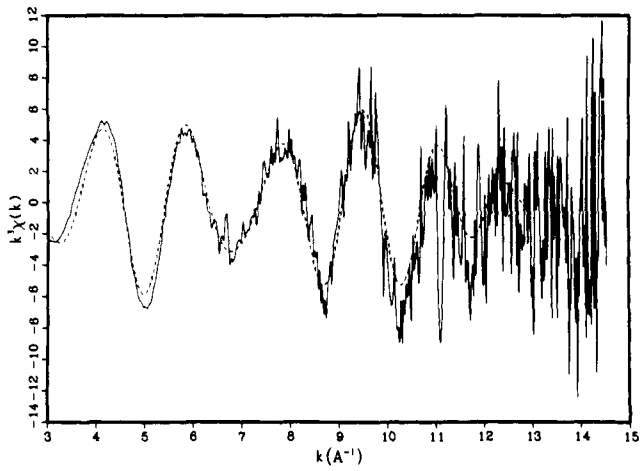

Figure 2. Unfiltered (solid curve) and Fourier filtered (dashed curve) $k^3\chi(k)$ vs. k EXAFS data of oxidized bacterial ferredoxin in solution.

moved by using a cubic spline technique containing three sections.[17a] The resulting $k^3\chi(k)$ data are shown as solid curves in Figure 2 for the oxidized bacterial ferredoxins. In addition to these reductions of the data, the $k^3\chi(k)$ vs. k data for the two model compounds $(Et_4N)_2^+[FeS(SCH_2)_2C_6H_4]_2^{2-}$ and $(Et_4N)_2^+[FeS(SCH_2Ph)]_4^{2-}$ were also corrected for the μ_0 dropoff via Victoreen's true $\mu_0/\rho = C\lambda^3 - D\lambda^4$ equation with $C = 126$ and $D = 27.2$ for iron.[18]

For the purpose of curve fitting, the high-frequency noise and the small residual background in each spectrum coming from distant neighbors were removed by a Fourier filtering technique.[17b] This involves Fourier transforming the $\chi(k)k^3$ data into R space, selecting the distance (R) range to be kept, and back transforming to k space. The resulting filtered data, subsequently truncated at 3 and 13 Å^{-1}, are compared (dashed vs. solid curves) with the unfiltered data in Figure 2 for the typical case of the oxidized bacterial ferredoxins. Data filtered in this way were used for the following curve fitting. Typical Fourier transforms of unfiltered EXAFS data are depicted in Figures 3a-d.

Least-Squares Refinements. We use the least-squares minimization technique to fit the filtered spectra wtih a multiple-term semiempirical expression of the EXAFS model. A nonlinear least-squares program, which utilizes Marquardt's scheme for iterative estimation of nonlinear least-squares parameters via a compromise combination of gradient (when far from minimum) and Taylor series (when close to a minimum) method,[19] was used. For the present systems which contain two different types of nearest neighbors (viz., four sulfurs and one iron in the dimer and four sulfurs and three irons in the tetramer), a two-term fit of the following expression was used:[16,20-24]

$$\chi(k)k^3 = N\left[N_S F_S(k_S) k_S^2 e^{-2\sigma_S^2 k_S^2} \frac{\sin\,[2k_S r_S + \phi_S(k_S)]}{r_S^2} + N_{Fe} F_{Fe}(k_{Fe}) k_{Fe}^2 e^{-2\sigma_{Fe}^2 k_{Fe}^2} \times \frac{\sin\,[2k_{Fe} r_{Fe} + \phi_{Fe}(k_{Fe})]}{r_{Fe}^2}\right] \quad (2)$$

The terms $F_i(k_i)$, $\phi_i(k_i)$, N_i, σ_i, r_i, and k_i denote the amplitude, the phase, the number of bonds, the Debye-Waller factor, the bond distance, and the photoelectron wave vector, respectively, of the ith type neighboring atom where i = S, Fe. The present length of the data set does not justify fitting with multiple iron-sulfur and/or multiple iron-iron (in the case of tetramers) distances since it has been shown that the smallest differences of distance Δr which can be distinguished from a least-squares fit are determined by the length of the data set by the relation $\Delta r \approx \pi/2k$.[8] Nevertheless, the Debye-Waller

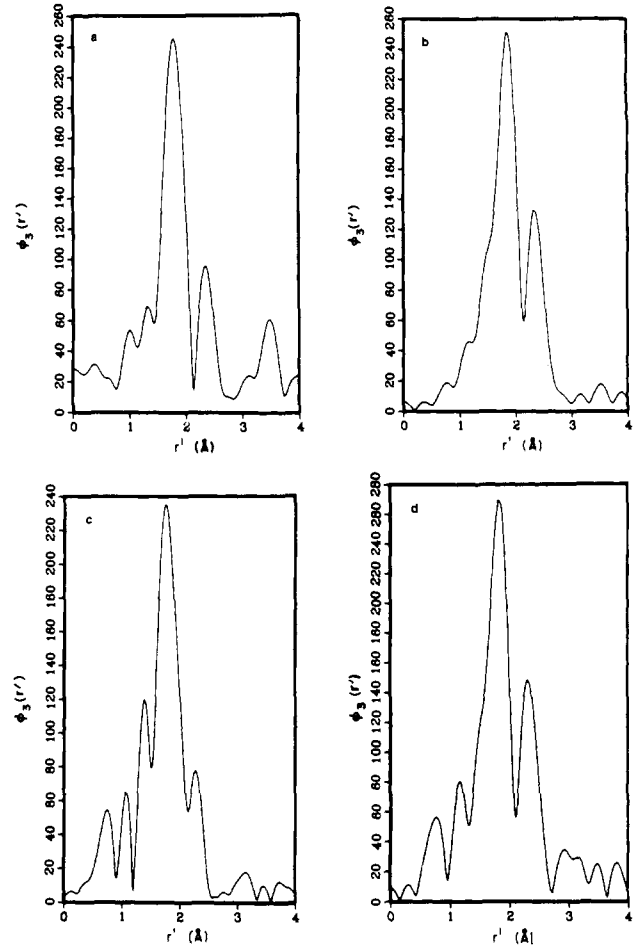

Figure 3. Fourier transforms of the $k^3\chi(k)$ data of (a) model dimer; (b) model tetramer; (c) oxidized plant ferredoxin (powder); (d) oxidized HIPIP (solution). Smooth filtering windows of 0.9-3.5 Å were used.[17c]

factors are good measures of the possible spread of nonequivalent distances.

For such a complex system it has been found impractical to vary the overall scale factor N, the amplitude functions, the number of bonds, the Debye-Waller factors, and the distances simultaneously even with a detailed knowledge of phase shifts. We therefore resort to the recently reported theoretical amplitude and phase functions and hold these parametrized functions,[15] as well as the number of bonds N_i, fixed in all our fitting procedures. The parametrized theoretical amplitude and phase functions are

$$F_i(k_i) = \frac{A_i}{1 + B_i^2(k_i - C_i)^2} \quad (3)$$

$$\phi_i(k_i) = P_{0_i} + P_{1_i}k_i + P_{2_i}k_i^2 + P_{3_i}/k_i^3 \quad (4)$$

where the parameters $\{A, B, C\}$ and $\{P_0, P_1, P_2, P_3\}$ were taken from the literature and listed in Table I. Since the phase functions are unique only when a particular energy threshold E_0 is specified, our choice of $E_0 = 7127$ eV may not be consistent with the theoretical E_0's for each of the different types of bonds for which the theoretical phase shift $\phi_i(k_i)$ is defined.[16,23] We therefore allow a different E_0 value for each type of bond via least-squares refining the difference ΔE_{0_i} (eV) = $E_{0_i}^{th} - E_0^{exp}$ in

$$k_i = \sqrt{k^2 - 2(\Delta E_{0_i})/7.62} \quad (5)$$

where k is the experimental wave vector with E_0^{exp} (=7127 eV) and k_i is the theoretical wave vector with $E_{0_i}^{th}$. Seven parameters are varied in the nonlinear least-squares refined

Table I. Theoretical Amplitude Parameters A (Å), B (Å) and C (Å^{-1}) and Phase Parameters P_0, P_1, P_2, and P_3 for Atom Pairs X–Y = Fe–S and Fe–Fe where X Is the Absorber and Y Is the Backscatterer

X-Y	Fe-S	Fe-Fe
A	0.783	0.656
B	0.237	0.194
C	3.40	6.35
P_0	0.258	2.268
P_1	−1.317	−1.222
P_2	0.0308	0.026
P_3	27.5	−50.5

curve fitting: the overall scale factor N, two Debye-Waller factors σ_S and σ_{Fe}, two distances r_S and r_{Fe}, and two threshold energy differences ΔE_{0S} and ΔE_{0Fe}. Figures 4a–d show typical fits (dashed curves) of this EXAFS model to the Fourier-filtered data (solid curves).

The resulting least-squares refined interatomic distances and the Debye-Waller factors, with estimated standard deviations, are listed in Table II.[25]

Results and Discussion

Table II lists the EXAFS and crystallographical (if available) results of iron-sulfur proteins and model compounds containing one, two, four, and eight iron atoms. EXAFS data on rubredoxin and its models were taken from our recent publication[8b] and included here for comparison.

It is gratifying to note from Table II that the EXAFS results are in excellent agreement with single-crystal X-ray structural data, especially for the model compounds (small clusters) where accurate crystallographic information is available. For protein systems where crystallographical data are available, EXAFS results generally fall in the range of bond lengths derived from the low-resolution electron density map (vide infra).

In the following paragraphs, we will first discuss in some detail the model compounds by comparing the EXAFS results with the X-ray crystallographic data. We will then compare the molecular parameters of the models with the proteins which provides strong structural evidence that these inorganic model compounds are excellent representations of the active sites of the proteins, in accord with previous studies. Finally, a detailed comparison of the structural parameters will be made between various phases (solid vs. solution), stereochemistries (monomer vs. dimer vs. tetramer), and oxidation states (oxidized vs. reduced).

1. Model Compounds. Table II shows that, in the model compounds **1**–**4**, the EXAFS results are accurate to better than 0.02 Å in Fe–S and 0.03 Å in Fe–Fe bond distances. These EXAFS values are based upon parametrized theoretical amplitude and phase functions which are known to give interatomic distances accurate to ca. 0.01–0.02 Å.[15,23] For the Fe–S bonds this accuracy is comparable to the errors introduced by fitting errors and the initial choice of energy threshold (E_0). This level of accuracy can be taken as confidence limits for the structural parameters determined for the proteins. For the Fe–Fe distances the fitting errors are larger than all these and are dominant.

The average Fe–S distances determined by EXAFS are 2.279 (13), 2.340 (14), 2.234 (15), and 2.270 (13) Å for $[Fe(S_2\text{-}o\text{-}xyl)_2]^-$ (**1**), $[Fe(S_2\text{-}o\text{-}xyl)_2]^{2-}$ (**2**), $[Fe_2S_2(S_2\text{-}o\text{-}xyl)_2]^{2-}$ (**3**), and $[Fe_4S_4(S\text{-}benzyl)_4]^{2-}$ (**4**), respectively. These values compare very well with those of 2.267 (2),[5a] 2.356 (5),[5a] 2.257 (2),[6] and 2.286 (2)[7a] Å determined by X-ray crystallography. Similarly, the average Fe–Fe distances of 2.704 (23) and 2.717 (24) Å found for **3** and **4**, respectively, by EXAFS are in excellent agreement with the corresponding values of

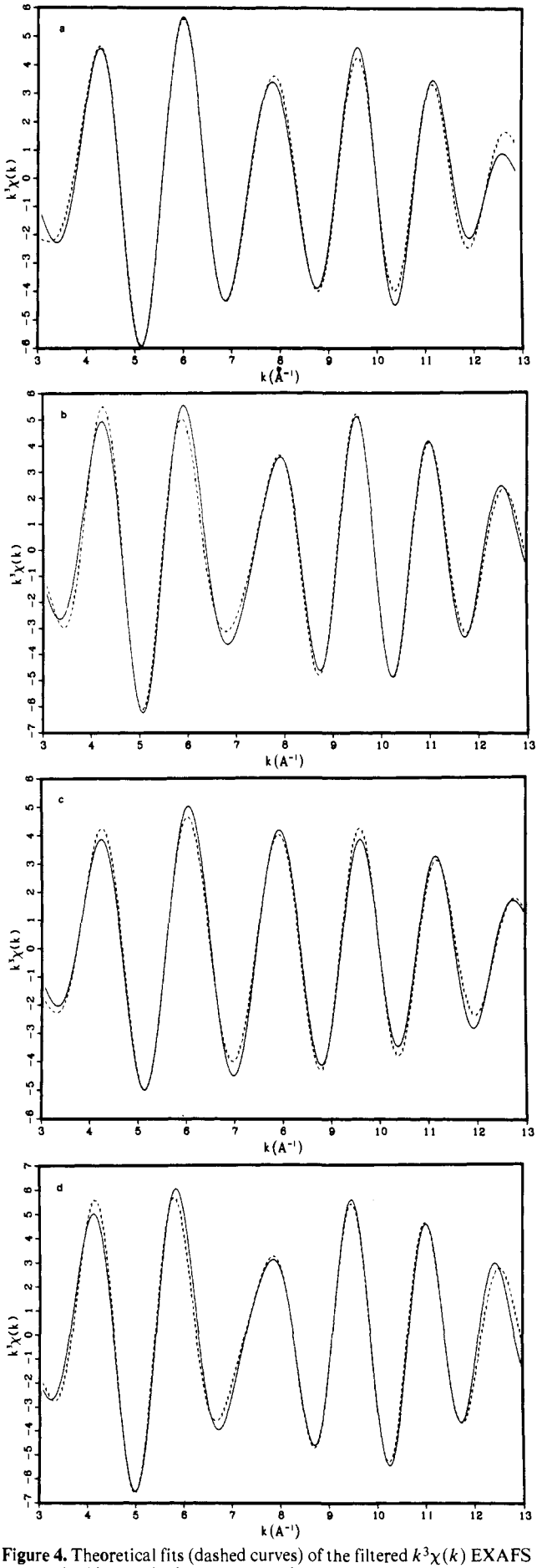

Figure 4. Theoretical fits (dashed curves) of the filtered $k^3\chi(k)$ EXAFS spectra (solid curves) of the same set of compounds listed in the caption of Figure 3a–d.

Table II. Least-Squares Refined Interatomic Distances (Å) and Debye-Waller Factors (Å) with Fitting Errors for Iron-Sulfur Models (**1**-**4**) and Proteins (**5**-**14**)[a-c] and Their Comparisons with Crystallographic Results (Bond Lengths Only)

no.	compd		EXAFS Fe-S	EXAFS Fe-Fe	diffraction Fe-S	diffraction Fe-Fe
			Model Compounds			
1	$[Fe(S_2\text{-}o\text{-}xyl)_2]^-$	r	2.279 (13)		2.267 (2)	
		σ	0.043 (15)			
2	$[Fe(S_2\text{-}o\text{-}xyl)_2]^{2-}$	r	2.340 (14)		2.356 (5)	
		σ	0.053 (17)			
3	$[Fe_2S_2(S_2\text{-}o\text{-}xyl)_2]^{2-}$	r	2.234 (15)	2.704 (23)	2.257 (2)	2.698 (1)
		σ	0.070 (11)	0.070 (10)		
4	$[Fe_4S_4(S\text{-}benzyl)_4]^{2-}$	r	2.270 (13)	2.717 (24)	2.286 (2)	2.747 (2)
		σ	0.064 (10)	0.093 (9)		
			Proteins			
5	Rub_{ox}(solid)	r	2.265 (13)		2.24	
		σ	0.049 (15)			
6	Rub_{ox}(soln)	r	2.256 (16)			
		σ	0.047 (18)			
7	Rub_{red}(soln)	r	2.32 (2)			
		σ	0.057 (25)			
8	plant Fd_{ox}(solid)	r	2.227 (15)	2.696 (47)		
		σ	0.063 (14)	0.078 (16)		
9	plant Fd_{ox}(soln)[d]	r	2.233 (22)	2.726 (40)		
		σ	0.063 (19)	0.057 (18)		
10	plant Fd_{red}(soln)[d]	r	2.241 (28)	2.762 (48)		
		σ	0.059 (22)	0.076 (31)		
11	$HIPIP_{ox}$(soln)	r	2.262 (13)	2.705 (26)	2.24 (5)	2.73 (4)
		σ	0.060 (11)	0.088 (9)		
12	$HIPIP_{red}$(soln)	r	2.251 (13)	2.659 (50)	2.30 (7)	2.81 (5)
		σ	0.001 (27)	0.088 (17)		
13	bact Fd_{ox}(soln)	r	2.249 (16)	2.727 (35)	2.27 (20)	2.85 (10)
		σ	0.063 (15)	0.092 (13)		
14	bact Fd_{red}(soln)	r	2.262 (14)	2.744 (32)		
		σ	0.062 (11)	0.098 (13)		

[a] Abbreviations: Rub, rubredoxin; Fd, ferredoxin; bact, bacterial; HIPIP, high-potential iron protein; ox, oxidized; red, reduced; soln, solution. [b] The fitting errors for each parameter (in parentheses) were obtained by changing that particular parameter, while least-squares refining the others within the same term, until the χ^2 contribution from that particular term is doubled. All parameters associated with the other term (except the overall scale factor) were held constant. [c] Other systematic errors including background removal and Fourier filtering may give rise to uncertainties of 1, 2, and 10% in r(Fe-S), r(Fe-Fe), and σ, respectively. [d] The data for **4** and **5** are poorer so that the errors should probably be doubled.

2.698 (1)[6] and 2.747 (2)[7a] Å determined by X-ray structural studies.

In our EXAFS analysis, no attempt was made to resolve the nonequivalent Fe-S or Fe-Fe distances owing to the limitations imposed by the data length which by the relation $\Delta r \approx \pi/2k$ limits our resolution to ≈0.15 Å, while X-ray diffraction studies of the models show that the spread of Fe-S or Fe-Fe distances is less than this. However, the Debye-Waller factors provide some indications about such spread of distances (if any) assuming that the vibrational contribution to the Debye-Waller factor is known well enough to be subtracted without lowering the accuracy. For a given type of atom pair with two sets (m and n) of nonequivalent distances the contribution to the Debye-Waller factor, σ_{stat}, due to this "static disorder" can be shown to be

$$\sigma_{stat} = \frac{\sqrt{mn}}{m+n}\Delta r \qquad (6)$$

where m bond distances are significantly different from n bond distances by Δr. This equation is derivable from $\sigma_{stat} \approx \delta = \sqrt{\sum^N (r-\bar{r})^2/N}$ where $N = m + n$, $\bar{r} = (mr_m + nr_n)/(m+n)$. Alternatively, it can be derived from the EXAFS expression

$$\chi(k) = F(k)e^{-2\sigma^2k^2}\left[\frac{m\sin(2kr_m + \phi(k))}{kr_m^2} + \frac{n\sin(2kr_n + \phi(k))}{kr_n^2}\right]$$

by combining the two terms in the bracket and by keeping terms to the order of δ^2k^2 for $k\delta \ll \pi$. The overall Debye-Waller factor, however, is determined by both the static variation of bond distances and thermal vibrations so that

$$\sigma^2 = \sigma_{stat}^2 + \sigma_{vib}^2 \qquad (7)$$

The values of σ can be determined by fitting the EXAFS spectra with eq 2; the results are in Table II. For the monomeric models **1** and **2**, we found the spread (Δr) of the Fe-S bond lengths to be 0.00 (4) and 0.06 (4) Å, respectively, if we assume an m:n = 2:2 model and a σ_{vib} of 0.045 Å (based on the Fe-S vibrational frequency of 314 cm^{-1}).[8b] These values are in good agreement with the X-ray crystallographic results of 0.00 (1) (range: 2.252 (2)-2.279 (2) Å) and 0.04 (1) Å (range: 2.324 (5)-2.378 (5) Å) for oxidized and reduced forms, respectively.[5a] For the oxidized forms of the dimeric (**3**) and the tetrameric (**4**) species, the Debye-Waller factors are 0.070 (11) and 0.064 (10) Å for the Fe-S bonds and 0.070 (10) and 0.093 (9) Å for the Fe-Fe bonds, respectively. Assuming for the Fe-S bonds a reasonable value of σ_{vib} = 0.045 Å, we calculated σ_{stat} = 0.054 and 0.046 Å which for a m:n = 2:2 model gives Δr(Fe-S) = 0.11 and 0.09 Å for **3** and **4**, respectively. These values are in good agreement with the corresponding crystallographic spreads of 0.10 and 0.07 Å, respectively.[6,7a] In **3**, single-crystal X-ray crystallographic study[6] revealed that the two terminal Fe-S bonds of 2.305 (av) Å are significantly (0.10 Å) longer than the two bridging Fe-S bonds of 2.209 (av) Å. In **4**, there is a slight but significant D_{2d} distortion in the

cubane-like iron-sulfur core resulting in eight bridging Fe-S bonds of 2.310 (av) Å being significantly longer than both the four bridging Fe-S bonds of 2.239 (av) Å and the four terminal Fe-S bonds of 2.251 (av) Å.[7a] In both **3** and **4**, therefore, the EXAFS data analyzed in terms of the *m:n* = 2:2 model works well even though in the latter compound the spread of distances presumably does not correspond to the separation of bridging vs. terminal Fe-S distances. Similar calculation can be performed on the Debye-Waller factors of Fe-Fe bonds. In **3**, there is only one iron-iron bond ($\sigma_{stat} = 0$); we have $\sigma_{vib} = \sigma = 0.070$ Å for the Fe-Fe bond. If we assume the same value for the Fe-Fe bonds in **4**, we obtain a σ_{stat} value of 0.061 Å. Since single-crystal structural studies[7a] revealed a slight but significant D_{2d} distortion resulting in two Fe-Fe distances being different from the other four, we can assume a *m:n* = 1:2 model such that $\sigma_{stat} = (\sqrt{2}/3)\Delta r$ and hence Δr(Fe-Fe) = 0.13 Å. This latter value is considerably higher than the corresponding crystallographical value 0.044 Å which results from two Fe-Fe distances of 2.776 (2) Å being significantly different from the other four of 2.732 (2) Å.[7a]

For Fe-Fe distances, the higher EXAFS values of Δr can be attributed to a combination of factors including the uncertainty in σ_{vib} and the relative insensitivity of the least-squares fit to this parameter. Furthermore, it should be noted that at this stage EXAFS provides no information about the sign of Δr or the assignment of distances.

2. Models vs. Proteins. The chemical and physical properties of Holm's iron-sulfur clusters **1**-**4** suggest that they are close representations of the redox centers of the nonheme iron-sulfur proteins. Our EXAFS results, augmenting the protein crystallographic studies, show that these inorganic complexes are excellent structural analogues of the active sites of the proteins. It should be pointed out that, though protein crystallography provides unequivocal stereochemical information which is vital for understanding the structure of these proteins, the individual bond lengths are determined less accurately than in the EXAFS studies owing to the intrinsically low resolution of protein crystallography.

The finding[8b] of an average Fe-S bond length of 2.265 (13) Å in powder rubredoxin (**5**) agreed extremely well with the corresponding values of 2.279 (13) and 2.267 (2) Å found by EXAFS and X-ray crystallography, respectively, for the model compound $[Fe(S_2\text{-}o\text{-xyl})_2]^-$ (**1**), strongly suggesting that **1** is an excellent structural model for the active site of oxidized rubredoxin. This value also agrees reasonably well with the average value of 2.24 (3) Å (2.05-2.34 Å) found by protein crystallography for oxidized rubredoxin.[3a-c] Based on the determined Debye-Waller factor of 0.049 (15) Å, the four Fe-S bonds are concluded to be chemically equivalent to within 0.04 (+0.06 or −0.04) Å for either 3:1 or 2:2 (*m:n*) models. However, for oxidized rubredoxin in the crystalline state, protein crystallography initially revealed two kinds of Fe-S bonds: three of normal bond lengths spread around the value of $R_3 = 2.30$ (3) Å and one unusually short bond with $R_1 = 2.05$ (3) Å.[3a-c] After preliminary EXAFS results showed[8a,9a] that all four Fe-S bonds are of equal lengths to within ±0.15 Å, refinements of a second set of crystallographic data give a revised set of distances in which $R_3 - R_1 = 0.10$ Å (L. H. Jensen, private communication). Now both methods agree that the four Fe-S bonds in rubredoxin in the solid state are within 0.10 Å of each other. This conclusion disagrees with the proposal[3a-c] (based on the reported extremely short Fe-S bond) that rubredoxin represents an entatic state with an energetically strained Fe-S bond.

For the oxidized plant ferredoxin in powder form (**8**) we found average Fe-S and Fe-Fe bond distances of 2.227 (15) and 2.696 (47) Å, respectively. These values are (within experimental errors) identical with the corresponding values of 2.234 (15) and 2.704 (23) Å found[6] for the dimeric iron-sulfur model compound $[Fe_2S_2(S_2\text{-}o\text{-xyl})_2]^{2-}$ (**3**), again suggesting that **3** is an excellent structural analogue of the active site of oxidized plant ferredoxin. Assuming an *m:n* = 2:2 model and $\sigma_{vib} = 0.045$ Å for the Fe-S bonds, we calculate $|R_2 - R_2'| = 0.09$ Å from the determined σ of 0.063 (14). This latter value is slightly smaller than the 0.11 Å found for model compound **3**, suggesting that the terminal Fe-S(Cys) and the bridging Fe-S* bond lengths are very similar to those in **3** and that the spread may be slightly smaller. The Debye-Waller factor of 0.078 (16) Å for the single Fe-Fe bond in **8** is very similar to that of 0.070 (10) Å in **3**, indicating that the Fe-Fe vibrational force constants are probably very similar.

For ferredoxin containing 4Fe-4S* clusters **11**-**14** (note that **11** and **12** contain one 4Fe-4S* cluster whereas **13** and **14** contain two), the Fe-S and Fe-Fe distances range from 2.249 (16) to 2.262 (14) and from 2.659 (50) to 2.744 (32) Å, respectively. These values agree with the corresponding values of 2.270 (13) and 2.717 (24) Å found by EXAFS for the model compound $[Fe_4S_4(S\text{-benzyl})_4]^{2-}$ (**4**).[7a] While this comparison suggests that **4** is a good structural representation of the redox centers of these proteins, it is not possible to assign the oxidation states because of the small differences in Fe-S and Fe-Fe distances observed upon reduction. However, extensive spectroscopic studies have established that **4** is a good synthetic analogue of reduced HIPIP (**12**) and oxidized ferredoxin (**13**).

3. Comparisons. It is of prime importance to compare structural parameters of closely related species with various phases (solid vs. solution), stereochemistries (monomeric vs. dimeric vs. tetrameric), and oxidation states (oxidized vs. reduced). This might allow us to correlate subtle structural variations with changes in physical and chemical properties which are vital in the basic understanding of the function of these proteins.

One advantage of EXAFS spectroscopy is its ability to determine structural parameters in solution. This gives us the opportunity to compare solid-state structures with solution structures. We find, however, little changes in the structural parameters upon dissolving the proteins in solution. As can be seen in Table II, the agreements are generally within one standard deviation for both Fe-S and Fe-Fe bonds. The Debye-Waller factors are also in fair agreement in the two phases. These findings, taken together, indicate that the active sites of the proteins undergo little, if any, structural changes in going from powder to solution. Solvation effects on the redox properties must, therefore, be mediated through the proteins (perhaps the tertiary structure) and not directly upon the active sites. In this context, it is important to note that the reduction of reduced HIPIP (**12**) to a superreduced state can only be accomplished by denaturing the protein in 80% DMSO/H_2O (but not in aqueous solution)[26] whereas such reduction can readily be carried out for the electronically equivalent model compound **4** to its trianion as well as the oxidized bacterial ferredoxin **13** to its reduced state **14**.

There are characteristic trends in the average structural parameters in going from the monomeric to the dimeric and tetrameric iron-sulfur clusters. For the series of model compounds **1**, **3** and **4** which have been characterized by X-ray crystallography, the average terminal Fe-S distance first lengthens from 2.267 (2) Å in **1** to 2.305 (2) Å in **3** and then shortens to 2.251 (2) Å in **4**, which bears no relation to the iron formal oxidation states, which go from +3 to +3 to +2.5. The average Fe-S(bridging) and Fe-Fe distances increase by 0.08 and 0.05 Å, respectively, in going from the dimer **3** to the tetramer **4**. The average Fe-S bond lengths determined by EXAFS for **1**, **3**, and **4** are 2.279 (13), 2.234 (15), and 2.270 (13) Å, respectively, while the Fe-Fe distances in **3** and **4** are 2.704 (23) and 2.717 (24) Å. Within the experimental accuracy there is no correlation between these bond lengths and

formal charges. The same trend was observed in the proteins: the average Fe-S distances are 2.265 (13) Å in **5**, 2.227 (15) Å in **8**, and 2.251 (13) Å in **12**, once again showing a dip in the dimer distances. The average Fe-Fe distances are determined less accurately. With the exception of **12** ($HIPIP_{red}$), which is 2.659 (50) Å, all the Fe-Fe distances are ~2.72 (4) Å. The distance in **12** agrees with all the others within experimental errors except that in **10** which was plant Fd_{red} and was 2.762 (48) Å, so that the combined errors do not quite allow for overlap. With these small spreads (compared to the possible errors) we feel that it would be premature to attach any significance to the changes observed in the Fe-Fe distances except to say that they all are in the region of 2.72 Å, and are in agreement with those determined by crystallography for the model compounds. We intend to obtain larger EXAFS data sets so that the Fe-Fe distances can be determined more accurately.

On the other hand, the Fe-S distances are determined accurately enough to see that first they agree very well with the model compounds and second the lengths are not correlated with formal charges. We believe that the small but characteristic Fe-S bond length variations observed in going from the monomeric to the dimeric to the tetrameric iron-sulfur cluster systems are consequences of different stereochemistries rather than results of differences in metal charges as implied by the formal oxidation states. In fact, similar trend of structural variation has been observed in "nonbonded" (with no net metal-metal bonding) clusters $(Ph_3P)_4Ag_2Br_2$ and $(Ph_3P)_4Ag_4Br_4$ where electronic effects are relatively unimportant.[27,28]

In the past[8] we have measured the monomeric FeS_4 center in rubredoxin and its model compounds. Fourier transforms of the data showed a single peak, corresponding to the Fe-S distance. In the present cases of the two and four iron centers, the Fourier transforms definitely show two peaks at distances corresponding to the Fe-S and the Fe-Fe distances (cf. Figures 3a-d). These peaks, however, are not fully resolved in distance space. The intensity of the Fe-Fe peak relative to that of the Fe-S peak in the dimer with one Fe-Fe bond is less than the corresponding value in the tetramer with three Fe-Fe bonds in the coordination sphere (cf. Figures 3a-d). The Fe-S and the Fe-Fe bonds both contribute appreciably to the absorption as indicated by the beating modes seen at $k \approx 7.5$ Å^{-1} in Figures 4a-d for the 2-Fe and 4-Fe systems. These beating modes are due to the interference between the Fe-S and the Fe-Fe waves and are consequently absent in the 1-Fe systems. The differences in the relative intensities observed in the Fourier transforms are also manifested in these filtered EXAFS spectra (cf. Figures 4a-d) in that there is a much greater interference in the 4-Fe vs. the 2-Fe clusters. It is clear that the present data allows us to differentiate among the three types of Fe-S complexes discussed here with zero (1-Fe), one (2-Fe), and three (4-Fe) iron neighbors. However, because of the interplay between the Debye-Waller factors and the numbers of bonds in the fit, better data are needed to determine the exact number of contributing pairs.

Since the most important biophysical property of these iron-sulfur proteins appears to be their redox properties, it is important to correlate structure changes, if any, with the redox behavior, within the accuracy of the present measurements.

For each structural type, there were small but significant structural changes observed at the active site(s) upon reduction. Our results show that the magnitude (per electron) of such variations, however, decreases in going from monomeric to dimeric and tetrameric iron-sulfur clusters presumably owing to the increasing number of Fe-S and Fe-Fe bonds involved for each electron transfer. Upon reduction, the average Fe-S bond length in rubredoxin increased from 2.265 (13) (powder) and 2.256 (16) (solution) to 2.32 (2) Å (solution). This significant increase of 0.06 Å in the Fe-S bonds can be correlated with the change of Fe(III) in the oxidized to Fe(II) in the reduced form. It is also comparable to that of 0.06 (EXAFS) or 0.09 Å (X-ray crystallography) observed in the model compounds (**1** → **2**). Accompanying the increase of the Fe-S bond lengths upon reduction, there was an increase in the spread of the four chemically equivalent distances as indicated by an increase in Debye-Waller factors which go from 0.043 (15) to 0.053 (17) Å in the model compounds (**1** → **2**) and 0.049 (15) (powder) or 0.047 (18) (solution) to 0.057 (25) Å in rubredoxins (**5** or **6** to **7**).

Confining our attention to the Fe-S distances, which have an accuracy between ±0.01 and ±0.02 Å, we can compare the three proteins in their oxidized and reduced forms. Upon reduction the Fe-S distance in plant Fd goes from 2.23 to 2.24 Å, in HIPIP from 2.26 to 2.25 Å, and in bacterial Fd from 2.25 to 2.26 Å. In all cases these changes are much smaller than the change of 0.06 (EXAFS) or 0.09 Å (crystallography) reported for $[Fe(S_2\text{-}o\text{-}xyl)_2]^-$. Nor do they reflect the change of 2.24 to 2.30 reported from the protein crystal structure of HIPIP, but they do agree with those results within the errors quoted. Although the EXAFS results on HIPIP show a decrease of 0.01 Å of the Fe-S bond upon reduction, it is well within the limits of error. However, all these Fe-S bond length changes observed are small when compared to those in the single iron center.

Correlated with the small Fe-S changes there are small changes of the Fe-Fe distances listed in Table II. However, the larger possible errors in these bond lengths make it impossible to say anything definite about their changes upon reduction except that they are definitely smaller than 0.1 Å.

The magnitudes of these EXAFS changes are in accord with the corresponding changes of +0.025 and +0.007 Å found for the reduction of the model dianionic tetramer (**4**) to its trianion.[31]

It is clear from our results that the changes in the average structural parameters of the redox centers of iron-sulfur proteins upon electron transfer are by no means drastic and are very similar to those of the model compounds and that the changes upon incorporation in the protein are also very small. Though EXAFS does not allow the determination of the sense of distortion of the Fe_4S_4 cube,[31] the small changes and spreads of Fe-S and Fe-Fe distances rule out any drastic structural distortion. It has been shown earlier[8a] from a consideration of Fe-S stretching force constants that a distortion of 0.05 Å corresponds to a strain energy of kT at room temperature. All of the differences between the model compounds and the proteins are smaller than this, so that any strain energy either from the protein or from reduction, stored in the Fe-S group, is negligible on this scale. The implication is that any strain energy, if present, lies within the polypeptide region (either through a localized or a delocalized mechanism) rather than being stored in the redox centers.

Acknowledgments. We thank N. A. Stombaugh, L. L. Anderson, and C. C. McDonald of E. I. du Pont de Nemours Central Research Department for kindly providing samples of the proteins used in this study. We are also grateful to P. A. Lee, P. Eisenberger, B. M. Kincaid, and A. L. Simons for valuable consultations.

References and Notes

(1) (a) Bell Laboratories; (b) Stanford Synchrotron Radiation Laboratory, Stanford, Calif.
(2) For an excellent review, see R. H. Holm, *Acc. Chem. Res.*, **10**, 427 (1977).
(3) (a) L. H. Jensen, *Annu. Rev. Biochem.*, **43**, 471 (1974); (b) K. D. Watenbaugh, L. C. Sieker, J. R. Herriot, and L. H. Jensen, *Acta Crystallogr., Sect. B*, **29**, 943 (1973), (c) L. H. Jensen, *Iron-Sulfur Proteins*, **2**, 163 (1973); (d) E. T. Adman, L. C. Sieker, and L. H. Jensen, *J. Biol. Chem.*, **248**, 4987 (1973); **251**, 3801 (1976); (e) E. Adman, K. D. Watenbaugh, and L. H. Jensen, *Proc. Natl. Acad. Sci. U.S.A.*, **72**, 4854 (1975).

(4) (a) C. W. Carter, Jr., *Iron-Sulfur Proteins*, **3**, 157 (1977); (b) T. Freer, R. A. Alden, C. W. Carter, Jr., and J. Kraut, *J. Biol. Chem.*, **250**, 46 (1975).
(5) (a) R. W. Lane, J. A. Ibers, R. B. Frankel, G. C. Papaefthymiou, and R. H. Holm, *J. Am. Chem. Soc.*, **99**, 84 (1977); (b) D. Coucouvanis et al., *ibid.*, **98**, 5721 (1976).
(6) J. J. Mayerle, S. E. Denmark, B. V. DePamphilis, J. A. Ibers, and R. H. Holm, *J. Am. Chem. Soc.*, **97**, 1032 (1975).
(7) (a) B. A. Averill, T. Herskovitz, R. H. Holm, and J. A. Ibers, *J. Am. Chem. Soc.*, **95**, 3523 (1973); (b) L. Que, Jr., M. A. Bobrik, J. A. Ibers, and R. H. Holm *ibid.*, **96**, 4168 (1974); (c) E. J. Laskowski et al., *ibid.*, **100**, 5322 (1978); (d) H. L. Carrell, J. P. Glusker, R. Job, and T. C. Bruice, *ibid.*, **99**, 3683 (1977).
(8) (a) R. G. Shulman, P. Eisenberger, W. E. Blumberg, and N. A. Stombaugh, *Proc. Natl. Acad. Sci. U.S.A.*, **72**, 4003 (1975); (b) R. G. Shulman, P. Eisenberger, B. K. Teo, B. M. Kincaid, and G. S. Brown, *J. Mol. Biol.*, **124**, 305 (1978).
(9) (a) D. E. Sayers, E. A. Stern, and J. R. Herriot, *J. Chem. Phys.*, **64**, 427 (1976); (b) B. Bunker and E. A. Stern, *Biophys. J.*, **19**, 253 (1977).
(10) (a) D. H. Petering and G. Palmer, *Arch. Biochem. Biophys.*, **141**, 456 (1970); (b) S. Kerestes-Nagy and E. Margoliash, *J. Biol. Chem.*, **244**, 5955 (1966).
(11) (a) R. G. Bartsch et al., *Methods Enzymol.*, **23**, 644 (1971); (b) L. E. Mortenson, R. C. Valentine, and J. E. Carnahan, *Biochem. Biophys. Res. Commun.*, **7**, 448 (1962).
(12) H. Winick in Proceedings of the IXth International Conference on High Energy Accelerators, Stanford Linear Accelerator Center, Stanford, Calif., 1974, pp 685–688.
(13) (a) P. Eisenberger, B. Kincaid, S. Hunter, D. Sayers, E. A. Stern, and F. Lytle in Proceedings of the Fourth International Conference on Vacuum Ultraviolet Radiation Physics, B. E. Koch, R. Haensel, and C. Kunz, Ed., Pergamon Press, Oxford, pp 806–807; (b) B. M. Kincaid, P. Eisenberger, and D. E. Sayers, to be published.
(14) J. Jaklevic, J. A. Kirby, M. P. Klein, A. S. Robertson, G. S. Brown, and P. Eisenberger, *Solid State Commun.*, **23**, 679 (1977).
(15) (a) B. K. Teo, P. A. Lee, A. L. Simons, P. Eisenberger, and B. M. Kincaid, *J. Am. Chem. Soc.*, **99**, 3854 (1977); (b) P. A. Lee, B. K. Teo, and A. L. Simons, *ibid.*, **99**, 3856 (1977); (c) B. K. Teo and P. A. Lee, *ibid.*, **101**, 2815 (1979).
(16) B. K. Teo, P. Eisenberger, and B. M. Kincaid, *J. Am. Chem. Soc.*, **100**, 1735 (1978).
(17) (a) A local cubic spline background removal program. (b) A local Fourier filtering routine developed by B. M. Kincaid. Application of Fourier filtering technique to EXAFS analysis has been done independently by Stern, Sayers, and Lytle. (c) See, for example, P. Eisenberger and B. M. Kincaid, *Science*, **200**, 1441 (1978).
(18) "International Table for X-ray Crystallography". Vol. III, Kynoch Press, Birmingham, England, 1968, pp 161, 1971.
(19) D. W. Marquardt, *J. Soc. Ind. Appl. Math.*, **11**, 443 (1963).
(20) E. A. Stern, *Phys. Rev., B*, **10**, 3027 (1974).
(21) (a) D. E. Sayers, E. A. Stern, and F. W. Lytle, *Phys. Rev. Lett.*, **27**, 1204 (1971); (b) F. W. Lytle, D. E. Sayers, and E. A. Stern, *Phys. Rev. B*, **11**, 4825 (1975); (c) E. A. Stern, D. E. Sayers, and F. W. Lytle, *ibid.*, **11**, 4836 (1975), and references cited therein.
(22) C. A. Ashley and S. Doniach, *Phys. Rev. B*, **11**, 1279 (1975).
(23) P. A. Lee and G. Beni, *Phys. Rev. B*, **15**, 2862 (1977).
(24) B. M. Kincaid and P. Eisenberger, *Phys. Rev. Lett.*, **34**, 1361 (1975).
(25) See footnotes *b* and *c* of Table II.
(26) R. Cammack, *Biochem. Biophys. Res. Commun.*, **54**, 548 (1973).
(27) B. K. Teo, and J. C. Calabrese, *J. Chem. Soc., Chem. Commun.*, 185 (1976).
(28) M. A. Bobrik, K. O. Hodgson, and R. H. Holm, *Inorg. Chem.*, **16**, 1851 (1977).
(29) W. R. Dunham, G. Palmer, R. H. Sands, and A. J. Bearden, *Biochim. Biophys. Acta*, **253**, 373 (1971).
(30) (a) C. W. Carter et al., *Proc. Natl. Acad. Sci. U.S.A.*, **69**, 3526 (1972); (b) C. W. Carter et al., *J. Biol. Chem.*, **249**, 6339 (1974).
(31) In going from $[FeS(SC_6H_5)]_4^{2-}$ to its trianion,[7c] the Fe_4S_4 core (of idealized D_{2d} symmetry in both cases) changes from a slightly compressed cubane-like structure (with eight long and four short Fe–S bonds of 2.296 (av) and 2.267 (av) Å, respectively) to a somewhat elongated configuration (with four long and eight short Fe–S bonds of 2.351 (av) and 2.288 (av) Å, respectively). This can be described in terms of an axial expansion along the $\bar{4}$ axis resulting in the elongation of the four short Fe–S bonds in the dianion by 0.08 Å to the four long ones in the trianion. On the other hand, the increases in average Fe–S and Fe–Fe distances, in going from the dianion to the trianion, amount to only 0.025 and 0.007 Å, respectively.

Neutron Diffraction Analysis of the Structure of $H_3Ni_4(C_5H_5)_4$

Thomas F. Koetzle,*[1a] Jörn Müller,*[1b] Donald L. Tipton,[1c] Donald W. Hart,[1c] and Robert Bau*[1c,d]

Contribution from the Department of Chemistry, Brookhaven National Laboratory, Upton, New York 11973, Institut für Anorganische und Analytische Chemie, Technische Universität Berlin, D-1 Berlin 12, West Germany, and the Department of Chemistry, University of Southern California, Los Angeles, California 90007.
Received March 19, 1979

Abstract: The structure of $H_3Ni_4Cp_4$ ($Cp = \eta^5$-C_5H_5), an unusual paramagnetic metal cluster complex, has been analyzed by single-crystal neutron diffraction techniques at low temperature (81 K). As predicted from an earlier X-ray diffraction study, the hydrogen atoms bridge three faces of the Ni_4 tetrahedral core. Although the Ni_4 cluster itself is an essentially undistorted tetrahedron [with Ni–Ni edges of 2.469 (6) Å], the individual Ni_3H linkages are unsymmetrical. The H atoms are slightly displaced away from the unique apical Ni atom: Ni–H distances involving the apical Ni atom average to 1.716 (3) Å, while those involving the basal Ni atoms average to 1.678 (6) Å. The overall mean Ni–H distance is 1.691 (8) Å, and the H atoms are situated an average of 0.907 (6) Å above the Ni_3 faces. Other average distances and angles in the molecule follow: H···H = 2.316 (6) Å, Ni–C = 2.132 (5) Å, Ni–H–Ni = 93.9 (3)°, H–Ni–H = 86.1 (6)°. The title compound crystallizes in space group $C2/c$ with the following cell parameters at 81 K: $a = 28.312$ (13) Å, $b = 9.234$ (5) Å, $c = 14.783$ (7) Å, $\beta = 103.35$ (2)°, $V = 3760$ (3) Å^3, $Z = 8$. The structure has been refined to yield final agreement factors of $R_F = 0.107$ and $R_{wF} = 0.067$ for 2616 reflections having $I > 1.5\,\sigma(I)$.

Introduction

Tetrakis(η^5-cyclopentadienyl)tetranickel trihydride is one of the few known examples of polynuclear organometallic complexes not containing carbonyl ligands. The compound was isolated from the reaction of CpNi(NO) ($Cp = \eta^5$-cyclopentadienyl) with $AlCl_3$ and $LiAlH_4$.[2] The presence of the three hydride ligands was inferred from the mass spectrum of the complex which showed ions resulting from the loss of one, two, and three H atoms. A particularly interesting aspect of $H_3Ni_4Cp_4$ is its electronic configuration. The unknown species Ni_4Cp_4 would have the expected "closed-shell" 60-electron configuration[3] and would be diamagnetic. Such a 60-electron species is in fact known as $H_4Co_4Cp_4$.[4] However, $H_3Ni_4Cp_4$ has three additional electrons which are all unpaired,[2] making the compound a rare example of a paramagnetic metal cluster complex. Spectral data give no indication of the presence of the hydride ligands,[2] but IR spectra frequently do not show absorptions due to stretching frequencies from bridging hy-

0002-7863/79/1501-5631$01.00/0 © 1979 American Chemical Society